Static Equivalent Model of Inverter-based Distributed Energy Resource for Fault Analysis of Power Distribution Grid

Dong-Eok Kim†, Namhun Cho, Seung-Kwon Yang

KEPCO Research Institute, Korea Electric Power Corporation, 105 Munji-Ro, Yusung-Gu, Daejeon, 34056, Korea
† dongeok9.kim@kepco.co.kr

Abstract

In this paper, we propose a method to develop a static equivalent model of an inverter-based distributed energy resource (DER), where the model is used for a steady-state fault analysis of a power grid. First, we introduce the characteristics of an inverter-based DER as well as its general configuration. Then, we derive the equivalent model of the DER on the basis of the characteristics. Last, the performance of the proposed method is proven by the results of computer simulations.

Keywords: Fault Analysis, Inverter-based Distributed Energy Resources, Static Equivalent Model

I. INTRODUCTION

Recently, various kinds of energy resources are integrated with advanced energy conversion technologies into the power grid. The equipment for energy conversion with power electronics is typically called a power converter. When a power converter is applied to convert DC power to AC power, it is called a DC/AC converter or, in another term, an inverter. These days, inverters are frequently used to integrate distributed energy resources (DERs) to the grid and the DERs including the inverters are named inverter-based DERs. The impact of DERs on the power grid has been discussed in several studies [1]-[4]. However, since inverter-based DERs are different in structure and control strategy from the conventional types of DERs integrated by synchronous generators (SGs) to the grid [5], their impact on the power grid requires a different approach and analysis.

The inverter for grid-integration converts DC to AC by chopping the DC voltage with a PWM technique; thus, it produces a large amount of switching noises. As the noise from an inverter-based DER to the power grid should be less than a certain amount, the inverter includes a comparatively large filter inductance to eliminate the noise [6], unlike conventional SG-based DERs having small internal impedances. In addition, the inverter uses feedback current control schemes for a stable power flow from the energy resource to the grid [7], especially for intermittently changing renewable energy resources. For these reasons, in [8][9], the authors suggested that an inverter-based DER is considered to be a current source when analyzing its effect on the power grid. However, the authors of [8][9] neither mentioned nor provided an accurate procedure of how the model of an inverter-based DER should be derived.

In this study, a method to develop an equivalent static model of an inverter-based DER is proposed. The equivalent model can be used for a steady-state fault analysis of a power grid with inverter-based DERs. We first introduce some features of an inverter-based DER, and then, based on the features, the equivalent model of the DER in the form of a current source is derived. To verify the validity of the proposed method, computer simulations are performed using MATLAB simulation tool. In the simulation test, we collect exact data from a complex dynamic simulation under a fault condition using MATLAB Simulink, and then we show the data is matched with those obtained by a fault analysis with the proposed method under the same fault condition.

II. FEATURES OF INVERTER-BASED DER

The features of a DER with an inverter system using a current control scheme are described in this section. Fig. 1 shows the configuration of an inverter-based DER, where each number in solid-line circle is associated with that in dotted-line circle. Fig. 1(a) shows the part of renewable generation, which consists of a renewable energy source and power converters. By ignoring the loss of the power converters, it can be assumed that the power captured from the renewable energy source (P_{RN0}) is fully transferred to the DC-link part, and the part of renewable generation can be simplified as a variable direct current source

$$I_{RN}(t) = P_{RN}(t)/V_{DC}(t) \tag{1}$$

where P_{RN} is the power generated from the renewable part and V_{DC} is the DC-link voltage. Fig. 1(b) shows the part of inverter system for grid-integration, which consists of DC-link part, a pack of power semiconductor switching devices, and LCL filters. The DC-link part generally includes DC capacitors and bypass resistors to resolve the power unbalance between P_{RN} and that flowing to the grid (P_{INV}). The DC voltage dynamics is expressed

$$\frac{dV_{DC}(t)}{dt} = \frac{1}{C_{DC}V_{DC}(t)}\left(P_{RN}(t) - P_R(t) - P_{INV}(t)\right) \tag{2}$$

where C_{DC} is the DC-link capacitance and P_R is the power dissipated by the bypass resistors. When V_{DC} remains constant ($\dot{V}_{DC} \approx 0$), it is expected that the power P_{RN} can be fully delivered to the grid through the inverter system unless $P_R \neq 0$. The pack

Manuscript received August 4, 2016, revised December 5, 2016, accepted December 6, 2016
ISSN 2465-8111(Print), 2466-0124(Online), DOI http://dx.doi.org/10.18770/KEPCO.2016.02.04.569

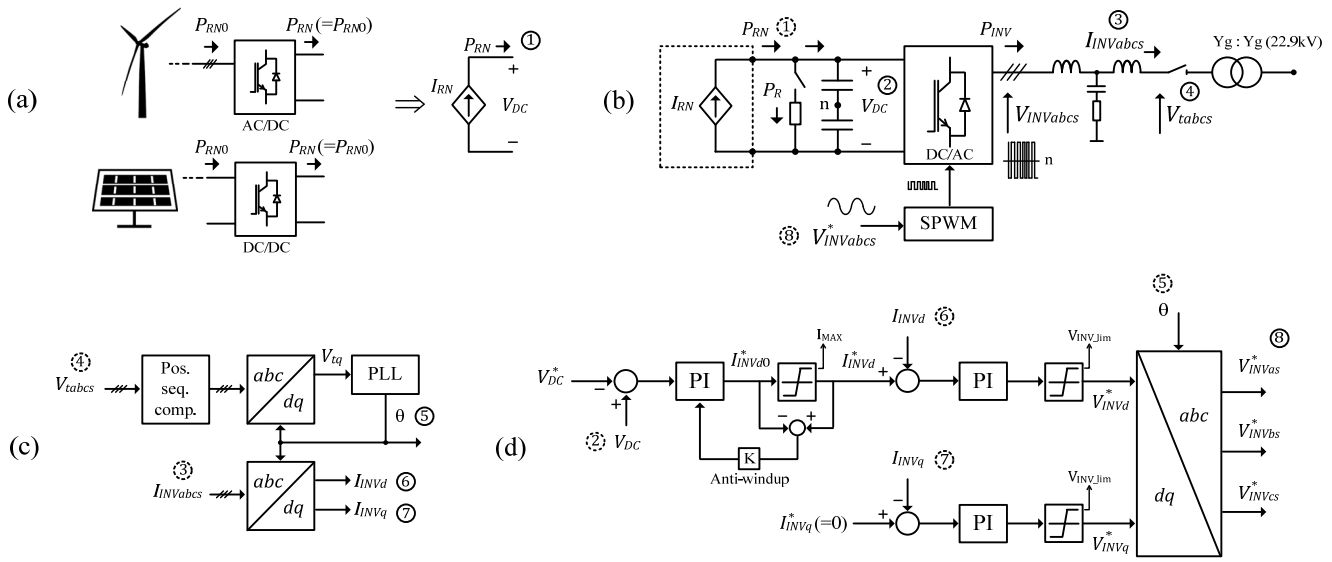

Fig. 1. Configuration of inverter-based DER. (a) renewable generation system. (b) inverter system for grid-integration. (c) PLL control. (d) control of DC-link voltage. and inverter currents.

of swithcing devices is called DC/AC converters whose role is to generate AC voltages ($V_{INVabcs}$) according to the given references ($V^*_{INVabcs}$) by chopping the DC-link voltage. The chopping process is basically carried out with a sinusoidal pulse-width modulation (SPWM) technique [10]. The output voltages of the DC/AC converters appear as chopped pulse waveforms which consist of the fundamental and switching frequency components on the basis of the DC-link neutral voltage. The LCL filters eliminate the switching frequency components so that the power related the fundamental frequency components is delivered to the grid. Fig. 1(c) and 1(d) show the control parts of the inverter system. Fig. 1(c) shows the part of phase-locked-loop (PLL) control [11] whose role is to generate the angle (θ) for *dq* transformation [12]. Three phase components are transformed to *dq* components with the transformation process. Fig. 1(d) shows the control part of the DC-link voltage and inverter currents. As mentioned, the DC-link voltage is controlled at a constant value by controlling the d-axis inverter current (I_{INVd}) while the q-axis inverter current (I_{INVq}) is controlled at zero for a unity power factor [13]. The current controller outputs (V^*_{INVd}, V^*_{INVq}), which are restricted by the limiters, are transformed to the three phase components ($V^*_{INVabcs}$) and those are used as the references for SPWM. In an analytic perspective of the fundamental frequency components, it can be assumed that the output voltages of the DC/AC converters are instantaneously the same to those of the controller outputs.

In the steady state of a normal condition, with the assumption of both P_{RN} and the inverter power (P_{INV}) being constant, it is expected that the d-axis current reference (I^*_{INVd}) is constant. On the other hand, in the steady state of a single-line fault condition, P_{INV} includes ripples due to the unbalanced grid condition, and thus V_{DC} includes small ripples as well by the power conservation between the power of DC-link capacitance P_{DC} ($E_{DC} = \frac{1}{2}C_{DC}V^2_{DC}$, $P_{DC} = \frac{t}{dt}E_{DC}$) and P_{INV} (assuming $P_R = 0$ and P_{RN} is constant). Then, the DC voltage controller produces its outputs (I^*_{INVd0}) to reduce the ripples in V_{DC} and this control action results in I^*_{INVd} having small ripples (mainly negative sequence components) unless I^*_{INVd0} is continuously larger than the value of the limiter (I_{MAX}). To make an equivalent modeling process easier, the small ripples in I^*_{INVd} will not be considered so that the current references are constant in both the steady state conditions.

III. EQUIVALENT MODEL FOR FAULT ANALYSIS

In order to analyze a fault occurred in a distribution grid with an inverter-based DER, we need to derive the symmetrical parts (positive, negative, and zero sequence parts) of an equivalent model of the DER. In this section, we explain how to derive the equivalent model from the perspective of the DER's characteristics.

A. Development of Equivalent Model

Fig. 2 shows the derivation of an equivalent model in the form of current source. Regarding LCL filters, as the filter capacitance is typically very small and the damping resistance is quite large, the current flowing into the capacitors is very small. Thus, for the steady-state analysis of the fundamental frequency, the capacitors and damping resistors can be ignored [6]. Then, the steady-state voltage equation for the filters is simply expressed with aggregated filter reactance X. In addition, the actual control of inverter current is performed with a reference I^*_{INV-} in the synchronous rotating frame generated with PLL technique. However, we will assume that the control is performed with the reference transformed ($I^*_{INV-} \rightarrow I^*_{INV}(= I^*_{INVd} + jI^*_{INVq})$) in a global rotating frame that is aligned with a given main voltage source. Note that I^*_{INV} includes only the direct components in the steady state. Then, an inverter system in Fig. 2(a) can be simplified to a *dq* (complex) model in Fig. 2(b).

Now, the inverter current is expressed,

$$I_{INV} = \frac{V_{INV} - V_t}{jX}, \quad \text{where} \quad I_{INV} = I_{INVd} + jI_{INVq}, \quad V_{INV} = V_{INVd} + jV_{INVq}, \text{ and } V_t = V_{td} + jV_{tq}$$

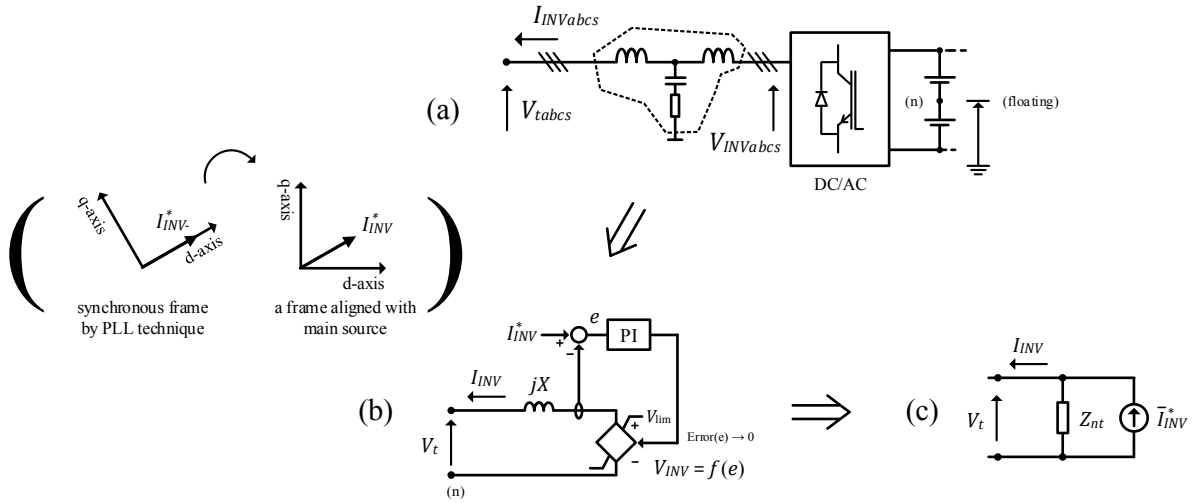

Fig. 2. (a) Inverter system. (b) simplified steady-state *dq* model of (a). (c) equivalent current source model of (b).

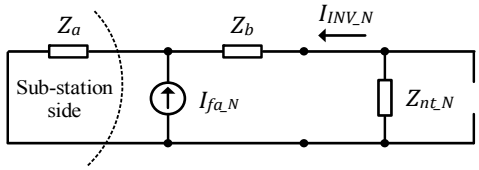

Fig. 3. Example of negative sequence circuit when a fault occurred.

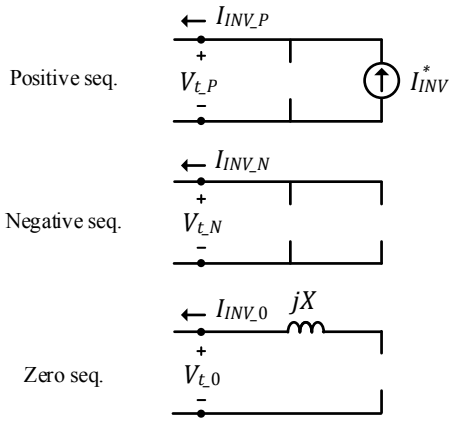

Fig. 4. Positive, negative, and zero sequence parts of the current source model in Fig. 2(c).

$$\bar{I}^*_{INV} = \frac{K(j\omega_c)}{K(j\omega_c)+jX} I^*_{INV} \text{ and } Z_{nt} = K(j\omega_c) + jX \tag{6}$$

Now, we need to derive the symmetrical parts of the current source model for fault analysis. Here, it is noted that ω of $X = \omega L$ is different from ω_c. ω represents the angular speed of a rotating frame but ω_c is for angular frequency components in that rotating frame. It needs to be noted that positive sequence components of 60 Hz in the stationary frame are expressed as direct (0 Hz) components in a frame rotating 377 rad/sec (60 Hz) in speed, while negative sequence components of 60 Hz in the stationary frame are expressed as 120 Hz components in that rotating frame. This implies that, while the gain effect of the controller for positive sequence is infinite ($K(j0) = \infty$), that for negative sequence is finite (large). From this implication, we conclude that 1) Norton impedance differs for the positive and negative sequences, and that 2) $\bar{I}^*_{INV}$ equals I^*_{INV}. In addition, we know that the zero sequence component of inverter current is not controlled and the inverter voltage is floating since DC-link neutral point is not grounded. Furthermore, from such an example shown in Fig. 3, we know that the negative sequence components of the inverter currents are determined by the fault current and the ratio of impedances

$$I_{INV\_N} = \frac{1}{Z_a+Z_b+Z_{nt\_N}} V_{s\_N}(=0) - \frac{Z_{nt\_N}}{Z_a+Z_b+Z_{nt\_N}} I^*_{INV\_N}(= 0) - \frac{Z_a}{Z_a+Z_b+Z_{nt\_N}} I_{fa\_N} \tag{7}$$

where I_{fa_N} is a fault current source in the negative sequence. From Eq. 7 and the fact of $Z_a \ll Z_{nt\_N}$, we know $I_{INV\_N} \approx 0$ (unless $I^*_{INV\_N} \neq 0$). Then, from the mentioned, it is concluded that $Z_{nt\_P,N} \approx \infty$ and, finally, we have the symmetrical parts of the current source model, as expressed in Fig. 4.

Fig. 5 shows an application example of the equivalent model for a single line-to-ground (SLG) fault analysis, where the fault current sources in the sequence circuits are all the same for SLG fault ($I_{fa\_P} = I_{fa\_N} = I_{fa\_0} = I_{fa}$); refer to [14][15], to study how to configure the suquence circuits by fault types and to calculate the fault current. Fig. 5(a) shows the single diagram of a

(3)

And, from PI control, we have an equation

$$K(j\omega_c)(I^*_{INV} - I_{INV}) = V_{INV}, \text{ where } K(j\omega_c) = K_P - j\frac{K_I}{\omega_c} \tag{4}$$

where K_P and K_I are the proportional and integral gains, respectively, of the PI controller. Substituting (3) into (4),

$$I_{INV} = \frac{K(j\omega_c)}{K(j\omega_c)+jX} I^*_{INV} - \frac{1}{K(j\omega_c)+jX} V_t \tag{5}$$

Using Eq. 5, we obtain a current source model with Norton impedance Z_{nt}, which is shown in Fig. 2(c)

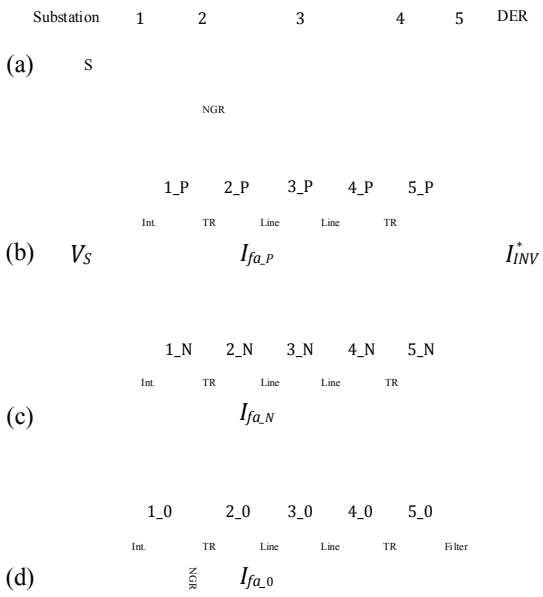

Fig. 5. (a) single diagram of a distribution grid with inverter-based DER, where single line-to-ground fault occurred. (b) – (c) symmetrical parts of (a) : (b) positive sequence. (c) negative sequence. (d) zero sequence.

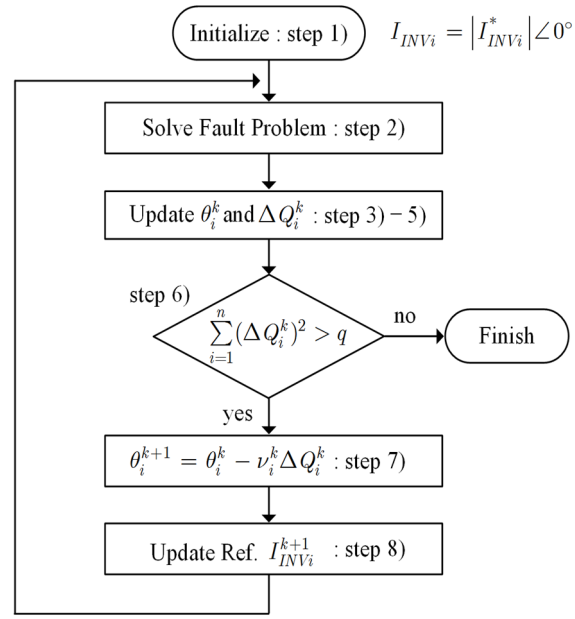

Fig. 6. Flowchart of the proposed method.

distribution grid with an inverter-based DER. A main voltage source (substation) with internal resistance is connected at bus 1 and the DER is connected at bus 5. It is assumed that fault occurred at node (bus) 3. Fig. 5(b)–(c) shows the symmetrical circuit parts of the distribution grid. A common fault analysis method described in [14] briefly is carried out in steps: 1) the symmetrical circuit parts without the fault current source are configured according to the types of faults and the fault current source I_{fa} is calculated accordingly. 2) After I_{fa} obtained, the symmetrical circuits with the fault current source are solved and the symmetrical components of bus voltages and currents are obtained. 3) the symmetrical components are transformed to the three-phase components.

B. Phase-Angle Correction of Equivalent Model

In this subsection, a method for adjusting the phase-angle of the current source model with an iterative process is presented. The flowchart of the process is shown in Fig. 6.

When DERs are integrated to the grid, they are generally controlled to achieve power factor 1 at their POCs (point of connections, in other words, terminals) with respect to the positive sequence components in both the normal and fault conditions. For this, we need to adjust the angles of the current source models, so that the angles are the same as those of the positive sequence components of the terminal voltages. The iterative process is stated below. Assuming that n DERs are interconnected with the grid,

1) Choose the magnitude of the current source model (reference) $|I^*_{INVi}|$, where the subscript i signify the number of DER (i^{th} DER). The initial angle of the reference is zero ($I^{*k}_{INVi} = |I^*_{INVi}|\angle 0°, \theta^k_{Ii} = 0, k = 1$).

2) Solve the fault problem and obtain the positive sequence components of the terminal voltages of the DERs.

3) Calculate a) the difference between the angles of V_{ti_P} and I^*_{INVi} and b) the reactive power at the DER terminal as

$$\theta_i^k = \theta_{Vi}^k - \theta_{Ii}^k, \tag{8}$$

where $\theta_{Vi}^k = \tan^{-1}\left(\frac{V_{ti\_Pq}^k}{V_{ti\_Pd}^k}\right)$, $\theta_{Ii}^k = \tan^{-1}\left(\frac{I_{INViq}^{*k}}{I_{INVid}^{*k}}\right)$, and

$$Q_i^k = \left|V_{ti\_P}^k\right|\left|I_{INVi}^{*k}\right| \sin\theta_i^k. \tag{9}$$

4) Calculate $\Delta Q_i^k = Q_i^k - Q_i^*$, where $Q_i^* = 0$ for power factor 1.

5) Stop if the squared sum of ΔQ_i^k is less than a predetermined value q. Otherwise, proceed to the next step.

6) Update the angle difference θ_i as

$$\theta_i^{k+1} = \theta_i^k - \nu_i^k \Delta Q_i^k, \tag{10}$$

where $\nu_i^k = \left|V_{ti\_P}^k\right|\left|I_{INVi}^{*k}\right| \cos\theta_i^k$. For stable convergence, $\nu_i^k \Delta Q_i^k$ is properly limited.

7) Update the reference I^*_{INVi} and go to 2):

$$I_{INVi}^{*k+1} = |I^*_{INVi}|(\cos\theta_{Ii}^{k+1} + j\sin\theta_{Ii}^{k+1}). \tag{11}$$

IV. SIMULATION RESULTS

To verify the performance of the proposed method, computer simulations are carried out using MATLAB tool. In simulation 1, the validity of the phase-angle correction method is proven. In simulation 2, exact data is first collected from a dynamic simulation under a fault condition using MATLAB Simulink, and then the fault analysis results calculated with the

Table 1. Reactive powers of DERs (current sources) in per-unit per iteration number (k=1, 7, 14)

DER no. \ Iteration	1	7	14
DER 1	0.0568	-0.0010	0.0000
DER 2	0.0413	-0.0003	0.0000
DER 3	0.0684	-0.0013	0.0000
DER 4	0.0684	-0.0013	0.0000
DER 5	0.0684	-0.0013	0.0000
DER 6	0.0490	-0.0004	0.0000
DER 7	0.0490	-0.0004	0.0000

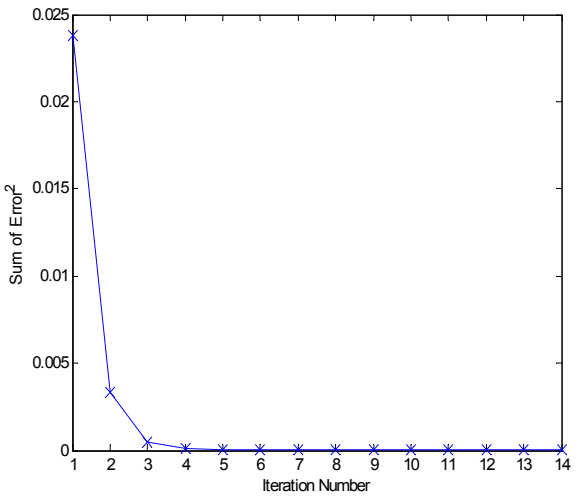

Fig. 7. Squared sum of $\Delta \boldsymbol{Q}_i^k$ through iteration process.

application of the equivalent model (will be called the proposed in this section) under the same fault condition are compared with those obtained from the dynamic simulation.

A. Simulation 1

The method of phase-angle correction is tested under a condition – 7 DERs are interconnected with a distribution grid and their currents are all set 0.1 per-unit (pu) in magnitude. The initial angles of the DERs are all zero on the basis of the angle of a main voltage source in the grid. In the process, $\left|v_i^k \Delta Q_i^k\right|$ is restricted within 0.01. The results are shown in Fig. 7 and Table 1. Fig. 7 shows $\sum\left(\Delta Q_i^k\right)^2$ is converging through the iteration process. Table 1 shows the reactive powers at the terminals of the 7 DERs, which all converge to zero (power factor 1).

B. Simulation 2

Now, in this subsection, the results of the proposed are compared with those obtained from a dynamic simulation using MATLAB Simulink. The model of a DER for the Simulink simulation was constructed as shown in Fig. 1 and Fig. 8. The rated power of the DER is 10 MW, and its inverter system consists of 10 "identical" 1 MW inverters connected to bus 5. The parameters of the 1 MW inverter used for the Simulink simulation are listed in Table 2.

The configuration of the distribution grid for the simulation is shown in Fig. 5(a), and the impedances are listed in Table 3. The base power is 100 MVA. The DER is operated at its rated power. The power factor at the terminal bus before the Y_g-Y_g transformer for grid integration is 1. In this work, the maximum

Table 2. Parameters of 1 MW inverter for the MATLAB Simulink simulation

		Parameters
DC/AC PWM Converter (Inverter for grid integration)		▪ LCL filters - (inv. side) $R_{f1} = 0.001\ \Omega$, $L_{f1} = 0.25$ mH - (grid side) $R_{f2} = 0.001\ \Omega$, $L_{f2} = 0.25$ mH - (filter cap. side) $C_f = 45\ \mu$F, $R_{fd} = 2\ \Omega$ ▪ DC-link capacitor: $C_{dc} = 30000\ \mu$F ▪ Sampling frequency: $f_s = 20$ kHz ▪ Switching frequency: $f_{sw} = 10$ kHz
Control	Ref. & limits	▪ DC-link voltage reference: $V_{dc}^* = 1060$ V (resistor switch turned-on if $V_{dc} > 1170$ V) ▪ DC-link voltage controller output's limit : $I_{MAX} = 215\ 0A_{peak}$ (1.0 pu) ▪ Current controller output's limit : $V_{INV\_lim} = 530\ V_{peak}$ (1.7 pu) ($V_{INV\_MAX} = 749.5\ V_{peak}$ (2.42 pu)) ▪ Inverter (line) voltage limit in (9) : $V_{lim(ll)} = 1165\ V_{peak}$ (2.167 pu)
	Gains	▪ Voltage controller gains - Proportional gain: $K_{P\_dc} = 2\zeta_{dc}C_{dc}\omega_{dc}$, - Integral gain: $K_{I\_dc} = C_{dc}\omega_{dc}^2$ ($\zeta_{dc} = 1$, $\omega_{dc} = 200$) - Anti-windup gain: $K = 1/K_{p\_dc}$ ▪ Current controller gains - Proportional gain: $K_P = 2\zeta_c L\omega_c$, - Integral gain: $K_I = L\omega_c^2$ ($\zeta_c = 0.707$, $L = L_{f1} + L_{f2}$, $\omega_c = 2500$)

Table 3. Impedance information of the distribution grid in Fig. 5 (a)

	Positive	Negative	Zero
Substation int. impedance	$j0.01$	$j0.01$	$j0.01$
Substation TR impedance (bus 1-2)	$j0.34$	$j0.34$	$j0.49$
Line impedances (bus 2-3, 3-4)	$0.1749 + j0.3876$	$0.1749 + j0.3876$	$0.45 + j1.14$
DER's TR impedance (bus 4-5)	$j0.60$	$j0.60$	$j0.60$
DER's filter impedance (jX)	$j13.5$	$j13.5$	$j13.5$

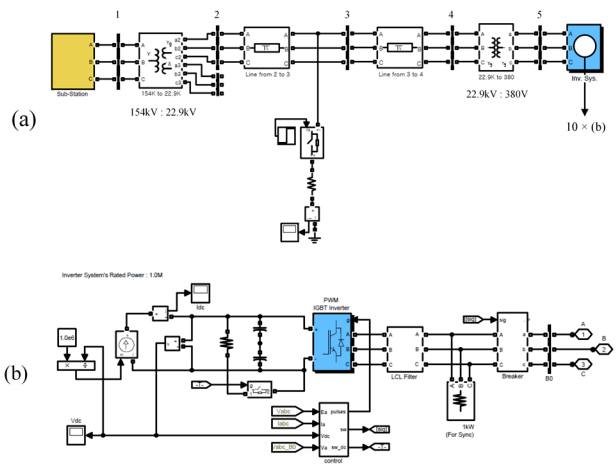

Fig. 8. (a) Simulink model of power system (S_B: 100 MVA) with 10 MW (10 × 1 MW) DER shown in Fig. 1. (b) Simulink model of 1 MW inverter-based DER.

current (I_{MAX} in Fig. 1(d)) of the DER is set to equal the rated value (0.1 pu). The terminal bus line voltage of the DER is 380 Vrms.

First, in the Simulink simulation, the control performance of the DER before and after a single-line fault is observed; before the fault, the DER injects its rated power to the grid through the

Table 4. Phase and symmetrical components of bus voltages on the basis of ground

Bus No.	Comp.	Matlab Simulink (a)		Proposed (b)		Error
		Mag. (p.u.)	Ang. (deg.)	Mag. (p.u.)	Ang. (deg.)	| a − b |
Bus 1	A	0.9938	-0.06	0.9938	-0.06	0
	B	0.9974	-119.83	0.9974	-119.82	0.0001
	C	0.9992	119.88	0.9992	119.88	0
	3Zero	0.0000	114.44	0.0000	-161.20	0
	Pos.	0.9968	0.00	0.9968	0.00	0
	Neg.	0.0032	-161.28	0.0032	-161.20	0
Bus 2	A	0.6495	-7.61	0.6495	-7.57	0.0004
	B	1.0286	-119.94	1.0290	-119.88	0.0011
	C	1.0050	124.51	1.0057	124.55	0.0009
	3Zero	0.4635	-161.21	0.4639	-161.20	0.0004
	Pos.	0.8914	-0.13	0.8918	-0.08	0.0008
	Neg.	0.1070	-161.28	0.1073	-161.20	0.0003
Bus 3	A	0.0004	-71.19	0.0000	-23.63	0.0004
	B	1.1732	-128.78	1.1736	-128.73	0.0010
	C	1.1909	136.39	1.1921	136.43	0.0014
	3Zero	1.5997	-176.65	1.6007	-176.64	0.0010
	Pos.	0.7691	3.89	0.7696	3.95	0.0009
	Neg.	0.2359	-174.80	0.2361	-174.72	0.0003
Bus 4	A	0.0423	77.10	0.0425	77.00	0.0002
	B	1.1770	-126.72	1.1775	-126.67	0.0011
	C	1.2121	138.13	1.2136	138.18	0.0018
	3Zero	1.5995	-176.66	1.6007	-176.64	0.0013
	Pos.	0.7824	6.87	0.7831	6.93	0.0010
	Neg.	0.2360	-174.83	0.2361	-174.72	0.0004
Bus 5	A	0.1000	91.56	0.1003	91.24	0.0006
	B	1.1598	-123.90	1.1604	-123.85	0.0011
	C	1.2205	140.90	1.2222	140.98	0.0024
	3Zero	1.5995	-176.67	1.6007	-176.64	0.0014
	Pos.	0.7798	11.26	0.7808	11.32	0.0012
	Neg.	0.2363	-174.85	0.2361	-174.72	0.0005

Table 5. Phase and symmetrical components of currents

Bus No.		Comp.	Matlab Simulink (a)		Proposed (b)		Error
From	To		Mag. (p.u.)	Ang. (deg.)	Mag. (p.u.)	Ang. (deg.)	| a − b |
S/S (0)	1	A	0.6305	-80.05	0.6259	-80.32	0.0054
		B	0.3986	100.80	0.3995	100.03	0.0054
		C	0.2320	98.49	0.2264	99.07	0.0060
		3Zero	0.0000	48.80	0.0000	-71.20	0
		Pos.	0.3223	-88.63	0.3183	-89.35	0.0056
		Neg.	0.3155	-71.28	0.3156	-71.20	0.0004
1	2	A	0.6305	-80.05	0.6259	-80.32	0.0054
		B	0.3986	100.80	0.3995	100.03	0.0054
		C	0.2320	98.49	0.2264	99.07	0.0060
		3Zero	0.0000	48.80	0.0000	-71.20	0
		Pos.	0.3223	-88.63	0.3183	-89.35	0.0056
		Neg.	0.3155	-71.28	0.3156	-71.20	0.0004
2	3	A	0.9390	-77.26	0.9388	-77.27	0.0002
		B	0.1000	71.33	0.1000	71.28	0
		C	0.0993	-48.57	0.1000	-48.72	0.0007
		3Zero	0.9460	-71.21	0.9466	-71.20	0.0006
		Pos.	0.3184	-89.30	0.3183	-89.35	0.0002
		Neg.	0.3157	-71.24	0.3156	-71.20	0.0002
5	4	A	0.1001	11.67	0.1000	11.28	0.0006
		B	0.1000	-108.67	0.1000	-108.72	0
		C	0.0993	131.43	0.1000	131.28	0.0007
		3Zero	0.0003	-6.94	0.0000	-75.58	0.0002
		Pos.	0.0998	11.47	0.1000	11.28	0.0003
		Neg.	0.0004	72.90	0.0000	24.29	0.0004
DER	5	A	0.1001	11.69	0.1000	11.28	0.0007
		B	0.1002	-108.72	0.1000	-108.72	0.0001
		C	0.0995	131.44	0.1000	131.28	0.0005
		3Zero	0.0000	164.85	0.0000	0.00	0
		Pos.	0.0999	11.47	0.1000	11.28	0.0003
		Neg.	0.0004	79.07	0.0000	0.00	0.0004

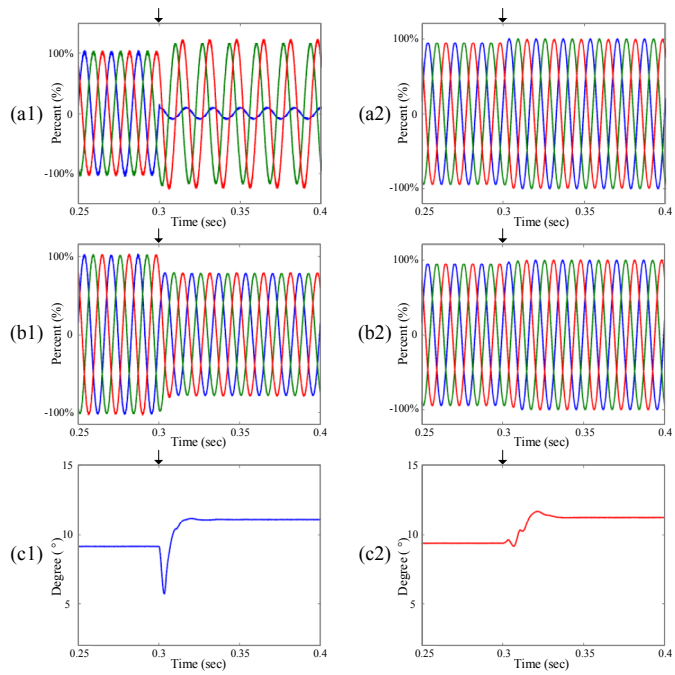

Fig. 9. (a1) 3 phase voltages at bus 5. (a2) 3 phase currents from bus 5 to the grid. (b1) positive sequence components of (a1). (b2) positive sequence components of (a2). (c1) A-phase angle of (b1). (c2) A-phase angle of (b2).

terminal bus and the fault occurred at 0.3 second. Fig. 9 shows the results; Fig. 9(a1) shows three phase voltages (on the basis of the ground) at bus 5 (DER's terminal bus) and Fig. 9(a2) shows three phase (inverter) currents flowing from bus 5 to the grid. Fig. 9(b1) and 9(b2) show the positive components of Fig. 9(a1) and 9(a2), respectively. Fig. 9(c1) and(c2) show the A-phase angles of the positive components shown in Fig. 9(b1) and 9(b2), respectively. It is observed that, before the fault, both the terminal voltages and currents are three-phase balanced; as the magnitude of the terminal voltage is little larger than 100 %, the magnitude of the current injected through the terminal bus is little smaller than 100% to meet the rated power (100%) under the condition of power factor 1 (the angles of the terminal voltages and currents are the same). After the fault at 0.3 second, the terminal voltages are unbalanced while the currents are still balanced. The positive sequence components of the terminal voltages are decreased to around 70% but the positive sequence components of the currents remain at 100% owing to the current limit, and thus the power injected to the grid is around 70%. Although it is not shown here, the rest 30% power is dissipated by the bypass resistors connected to the DC-link. In addition, it is observed that the A-phase angles of the positive sequence components of the terminal voltages and currents are changed after the fault, but they converged to the same (power factor 1).

Now, we compare the results of the proposed with those obtained from the Simulink simulation. For this, we collected the data of waveforms from the Simulink simulation and then processed them to obtain the phase and symmetrical components of the bus voltages and line currents. The results are written in Table 4 and 5, where all the angles are referenced on the basis of the main source voltage V_s $(1.0\angle 0°)$ in Fig. 5(b). The values from the proposed are accurately matched with those obtained from the Simulink simulation. In addition, it is noted that the angles of the positive components of the voltages of bus 5 in Table 4 are almost the same to those of the currents from DER to bus 5 in Table 5.

By all the results in the simulation section, it is confirmed that the proposed method is valid.

V. CONCLUSION

In this work, we proposed an equivalent model for a power system fault analysis. On the basis of the characteristics of an inverter-based DER including PI control scheme, we derived the simplified model of the DER and further equivalently reduced it to a model in the form of current source. The validity of the proposed was proven through computer simulations. However, we recall that the proposed does not include the effect of the inverter voltage limit, and thus it should not be used for a fault analysis when DERs run in the islanded mode. On the other hand, we believe that the proposed is expected to be useful for a better fault analysis for a power grid with inverter-based DERs. Our next work is to develop an equivalent model including the effect of the inverter voltage limit.

REFERENCES

[1] B. Kroposki, R. Lasseter, T. Ise, S. Morozumi, S. Papathanassiou, and N. Hatziargyriou "Making microgrids work," *IEEE Power and Energy Magazine*, vol. 6, no. 3, pp. 40-53, May–Jun. 2008.

[2] A. K. Basu, S. P. Chowdhury, S. Chowdhury, and S. Paul, "Microgrids: Energy management by strategic deployment of DERs—A comprehensive survey," *Renewable and Sustainable Energy Reviews*, vol. 15, no. 9, pp. 4348-4356, Dec. 2011.

[3] B. Kroposki, R. Margolis, G. Kuswa, J. Torres, W. Bower, T. Key, and D. Ton, "Renewable systems interconnection - executive summary," Technical Report, National Renewable Energy Laboratory, NREL/TP-581-42292, Feb. 2008.

[4] Th. Boutsika, S. Papathanassiou, and N. Drossos, "Calculation of the fault level contribution of distributed generation according to IEC Standard 60909," CIGRE Symposium Athens, Apr. 2005.

[5] J. A. Carr, J. C. Balda, and H. A. Mantooth, "A survey of systems to integrate distributed energy resources and energy storage on the utility grid," IEEE Energy 2030 Conference, Atlanta, Nov. 2008.

[6] M. Liserre, F. Blaabjerg, and S. Hansen, "Design and control of an LCL-filter-based three-phase active rectifier," *IEEE Trans. Ind. Applicat.*, vol. 31, no. 5, pp. 1281-1291, Sept. 2005.

[7] M. Prodanović and T. C. Green, "Control of power quality in inverter-based distributed generation," IEEE IECON, Nov. 2002, vol. 2, pp. 1185-1189.

[8] Advanced-Energy Inc., "Neutral connections and effective grounding," White Paper, 2013. Available: http://solarenergy.advancedenergy.com/upload/File/White_Papers/ENG-TOV-270-01%20web.pdf.

[9] L. Wieserman and T.E. McDermott, "Fault current and overvoltage calculations for inverter-based generation using symmetrical components," IEEE Energy Conversion Congress and Exposition, Sept. 2014, pp. 2619-2624.

[10] D.-W. Chung, J.-S. Kim, and S.-K. Sul, "Unified voltage modulation technique for real-time three-phase power conversion," *IEEE Transactions on Industry Applications*, vol. 34, no. 2, pp. 374-380, Mar./Apr. 1998.

[11] V. Kaura and V. Blasko, "Operation of a phase locked loop system under distorted utility conditions," *IEEE Transactions on Industry Applications*, vol. 33, no. 1, pp. 58-63, Jan./Feb. 1997.

[12] Y. Ohta, A. Ohori, N. Hattori, and K. Hirata, "Controller design of a grid-tie inverter bypassing DQ transformation," 52nd IEEE Conf. on Decision and Control, Dec. 2013, pp. 2927-2932.

[13] H.-S. Kim, J.-W. Baek, J. Cho, J. Kim, and J. Kim, "Output voltage balancing methods of 3-level NPC rectifier for low voltage DC distribution," 9th International Conference on Power Electronics and ECCE Asia, Jun. 2015, pp. 2539-2544.

[14] A. R. Bergen and V. Vittal, *Power System Analysis: 2nd Edition.* NJ, USA; Prentice-Hall, 2000.

[15] D.-E. Kim and N. Cho, "Fault analysis method for power distribution grid with PCS-based distribution energy resources." *Journal of Electrical Engineering and Technology* (To be published)